# "Seismic Performance of Strength Degraded Structures"

Rupali S Bhamare[1], Bidur Kafle[2], Nelson Lam[3], John Wilson[4], Emad Gad[5]

1. PhD student, Dept of Civil and Environmental Engineering, The University of Melbourne, VIC 3010, Australia. Email: bhamarer@unimelb.edu.au

2. PhD student, Dept of Civil and Environmental Engineering, The University of Melbourne, VIC 3010, Australia. Email: b.kafle@pgrad.unimelb.edu.au

3. Associate Professor and Reader, Dept of Civil and Environmental Engineering, The University of Melbourne, VIC 3010, Australia. Email: n.lam@civenv.unimelb.edu.au

4. Professor, Faculty of Engineering and Industrial Science, Swinburne University of Technology, Hawthorne, VIC 3122, Australia. Email: jwilson@groupwise.swin.edu.au

5. Assistant Professor, Dept of Civil and Environmental Engineering, The University of Melbourne, VIC 3010 and Faculty of Engineering and Industrial Science, Swinburne University of Technology, Hawthorne, VIC 3122, Australia. Email: egad@groupwise.swin.edu.au

**ABSTRACT:**

Traditionally, performance assessment of a structure is based on trading off strength demand with ductility demand. In high seismicity region, the design provisions are based on the concept of conservation of energy; such guidelines (FEMA 273) recommend a very low drift capacity for strength degraded structures. Furthermore, the application of these guidelines, results in most of the strength degraded structures deemed unsafe when subjected to earthquake excitations in low and moderate seismic regions. This paper presents results of nonlinear time history analyses (THA) for such strength degraded structures for a range of near-field and far-field earthquake scenarios of different M-R combinations. Fragility curves defining probability of failure of structures have been developed. The insensitivity of the probability of failure of the URM wall on its height (i.e. vertical span length) is an interesting finding in this study. Also, the extent of strength degradation in an unreinforced masonry wall is not shown to have increased its probability of failure.

**KEYWORDS**: Earthquake, displacement controlled behaviour, non linear time history analyses, strength degraded structures.

## 1 INTRODUCTION

Seismic design and assessment of structures have been based on trading-off strength with ductility demand to ensure that the structure has adequate energy dissipation capacity. In high seismic region, structures are deemed to be seismically unsafe if their energy dissipation capacity is exceeded by the energy demand from an earthquake. Structures in high seismic regions would need to be designed and detailed for ductile performances in order that they could accommodate large displacements without significant lateral strength degradation. Furthermore, when such standards are applied in low and moderate seismic regions, most of the strength degraded structures would be deemed to be seismically unsafe during earthquake excitations. For structures which have not been designed for seismic resistance namely rigid body objects, unreinforced masonry structures (URM) and soft-storey building, low drift capacity is recommended (ATC 40, FEMA 273) in view of their potential strength degradation behaviour.

However in low and moderate seismic regions, velocity demand subsides as the natural period increases. Importantly, the diminishing energy phenomenon indicates that the displacement demand on a structure is insensitive to the natural period as the displacement demand is constrained to an upper limit (Lam et al., 2005). Consequently the seismic performance of a structure can be controlled by its displacement capacity as opposed to its energy dissipation capacity. According to this phenomenon, structures are deemed seismically safe, if their displacement capacity exceeds the imposed displacement demand irrespective of their strength and energy dissipation capacity. Therefore this new assessment approach based on displacement controlled phenomena should be very much suited to low and moderate seismic regions where structures with strength degrading property are very common.

In order to by-pass conventional force based analysis which is time consuming, the new displacement controlled phenomena has been used to evaluate factors which can be used as the quick assessment of structures for design purposes. The single degree of freedom (SDOF) systems representing strength degraded structures are subjected to nonlinear time history analyses (THA) using simulated accelerograms on various soil sites. The simulations were based on a range of earthquake scenarios defined by magnitude epicentral distance (M-R) combinations. Most importantly, earthquake combinations include near-field and far-field earthquakes. The main aim of this study is to identify factors which can be applied in seismic design practices (for quick assessment of strength degraded structures). The seismic performance of structures can be assessed simply by comparing the displacement demand with the displacement capacity of a structure. The proposed method will result in significant savings in time and can easily by-pass conventional force based approach for seismic assessment. Interesting results from the parametric study have shown that probability of failure (POF) of a wall is not very sensitive to the height of the wall whereas the POF is dependant on the thickness of the wall and its strength degradation behaviour is shown to have not increased the chance of overturning.

Strength degradation and nonlinear force displacement relationship of these structures are described in Section 2. Various accelerograms with different M-R combinations employed for the analyses are described in Section 3. The maximum displacement demand of SDOF systems can be obtained from the elastic response spectra calculated for linear elastic systems (refer Section 4). Non linear time history analyses have been undertaken by the author(s). Fragility curves defining POF have been developed to study the seismic performance of strength degraded structures in displacement controlled conditions (refer Section 5).

## 2 STRENGTH DEGRADED STRUCTURES

### 2.1 *Rigid body objects (RBO)*

Rigid body objects (RBO) are free standing structural assemblies. When such structures are excited beyond the linear elastic range, the joints between the elements (or elements and the ground) will open and leave the blocks to rock about the pivotal edges (Figure 1). Some typical examples of systems which exhibit the rocking behaviour are tombstones, monumental columns, and free standing objects. The force-displacement relationship of rigid body rocking is generally represented by the vertical line (a-b) which denotes infinite initial stiffness, and negative slope (b-c) showing the degradation in strength as displacement increases (Figure 1). The force-displacement relationship of rigid objects exhibits non-linear elastic behaviour as the behaviour of loading, unloading and reloading is similar. This indicates that objects possess excellent self-centering capabilities under gravitational loading (Al Abadi et al., 2006).

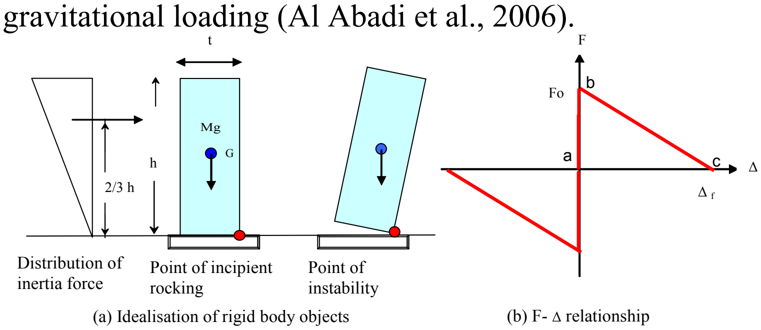


Figure 1. Force displacement relationship of rigid body objects.

### 2.2 *Unreinforced masonry structures (URM)*

Australia has a huge brick masonry building stock as compared to structures built from other construction materials. However, major limitation with URM structures is their vulnerability to earthquake loading due to limited ductility; URM structures are also heavy and brittle with low tensile strength. As a result, URM structures are vulnerable in areas of high seismicity. URM walls subjected to one-way bending, often respond in a non-linear, fully elastic manner. These systems have excellent self-centering capabilities as the displacement always reverts back to zero at each unloading or reloading cycle. However, there is very little energy dissipation during deformation of the walls. The force-displacement relationship is similar to that of a free-standing object, featuring significant strength degradation and no energy dissipation (Figure 2). When subjected to horizontal bending, a URM wall responds in a non-linear inelastic manner featuring significant strength degradation but showing energy dissipation capability due to friction (Doherty et al., 2002). For analyses purpose, semi rigid rocking model has been considered as it represents the real behaviour of a structure. The parameters defining semi rigid rocking model (i.e. $\Delta_1, \Delta_2$) are calculated from the ratio of $\Delta_1$ and $\Delta_f$ & ratio of $\Delta_2$ and $\Delta_f$ (Lam et al., 2003). Refer also Table 1.

Once height (h), thickness (t), $\Delta_1, \Delta_2$ and $\Delta_f$ are known, the tri-linear force displacement model can be readily used for the analyses; where initial stiffness is controlled by $\Delta_1$ and strength degradation is controlled by $\Delta_2$. The wall defining strength degraded conditions have also been taken into considerations. The terminology “new” refers to newly constructed walls, whereas the terminology “moderate” and “severe” refers to moderately degraded and severely degraded walls respectively (Doherty et al., 2002).

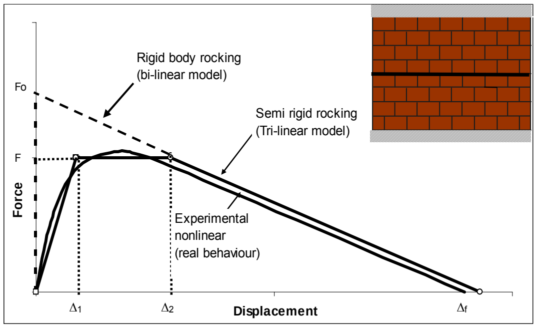


Figure 2. Tri linear force displacement relationship of URM.

| Table 1: Parameters of semi-rigid rocking model | | | | | | |
|---|---|---|---|---|---|---|
| Condition | $\frac{\Delta_1}{\Delta_f}$ (%) | $\frac{\Delta_1}{\Delta_f}$ (%) | Wall thickness (t)= $\Delta_f$ = 110mm | | Wall thickness (t) = $\Delta_f$ = 230mm | |
| | | | $\Delta_1$ (mm) | $\Delta_2$ (mm) | $\Delta_1$ (mm) | $\Delta_2$ (mm) |
| New | 6 | 28 | 7 | 30 | 14 | 65 |
| Moderate | 13 | 40 | 15 | 44 | 30 | 92 |
| Severe | 2 | 50 | 22 | 55 | 46 | 115 |
| New: New condition; Moderate: Moderately degraded structures; Severe: Severely degraded structures | | | | | | |

## 2.3 *Soft storey structures (SSC)*

Building structures possessing vertical stiffness irregularity with an open plan on the ground floor are very common. To utilise open space on the ground floor, the ground floors are free of structural walls. These buildings behave like an inverted pendulum in an earthquake. The columns in the open ground storey are often susceptible to severe damage, which may even lead to complete collapse of the building. An experimental program has been undertaken at The University of Melbourne to investigate the force-displacement behaviour of soft-storey columns under cyclic loading (Rodsin *et al.*, 2004). Two half-scaled reinforced concrete column specimens have been tested. The span-depth ratios of columns were deliberately considered as 3.75 (column S1) and 2.75 (column S2) so that the columns can undergo flexural and shear behaviour, respectively (Figure 3). Both columns were designed according to the Australian Standard (AS3600, 2001), (i.e. not designed for seismic loading). The tests were terminated at the incipient collapse of columns (when the columns had lost their axial load capacities) as opposed to the conventional 20% degradation of lateral strength (Figure 4).

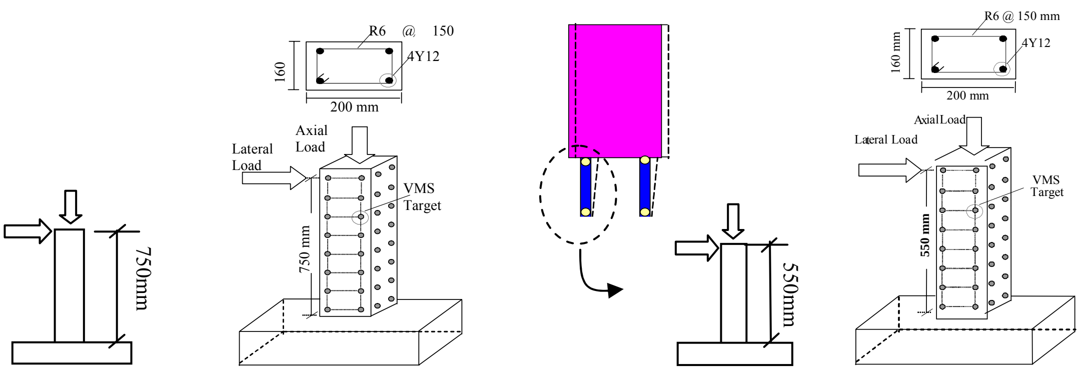


(a) (b)

Figure 3. Configuration of column S1 and S2 (Rodsin *et al.*, 2004) (a) Flexure dominated column (b) Shear dominated column.

Details of the test results have been reported in the paper by Rodsin et al. (2006) which was presented in the ACMSM conference. Classical hysteretic models have been calibrated to match with the experimental test results. The calibrated models have been used as input into the non linear time history analyses. Program RUAUMOKO (Carr, 2003) has been used for the seismic analyses (section 5.3). The capacities observed from the test are used to determine the state of failure for soft storey columns.

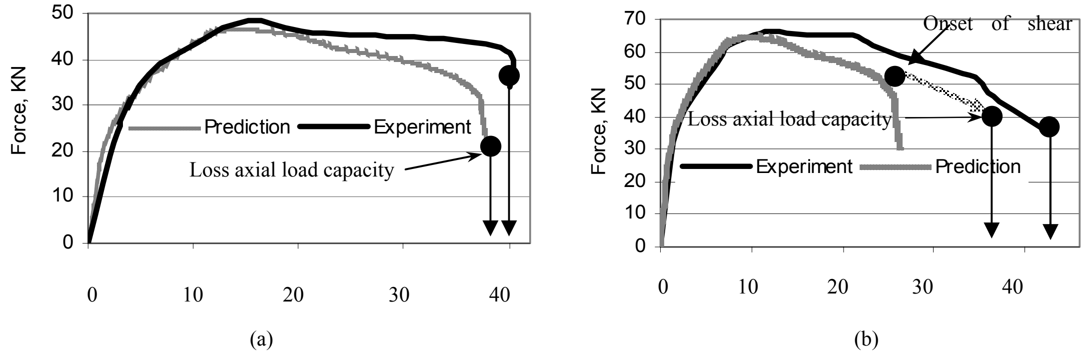


Figure 4. Force displacement curve from experimental test (a) Flexure-dominated Column, (b) Shear-dominated column.

## 3 APPLIED EXCITATION

The accelerograms for nonlinear time-history analyses (THAs) were generated by stochastic simulations of seismological models using program GENQKE (Lam et al., 2000) and SHAKE (Idriss et al., 1992). The simulations comprise various earthquake scenarios for different magnitude and epicentral distance combinations. The combination includes far-field and near-field earthquakes. By keeping the magnitude of the earthquake at 7 epicentral distances were varied from 177 Km to 14 Km on site class D which has a natural period of 0.89 sec (as per AS1170.4-2007 classification). Some 30 number of M7-R combinations were incorporated into the parametric studies.

Figure 5 shows a range of magnitude-distance combinations on the same soil site. To investigate the seismic performance of strength degraded structures, the earthquake scenarios presented in figure 5 were considered.

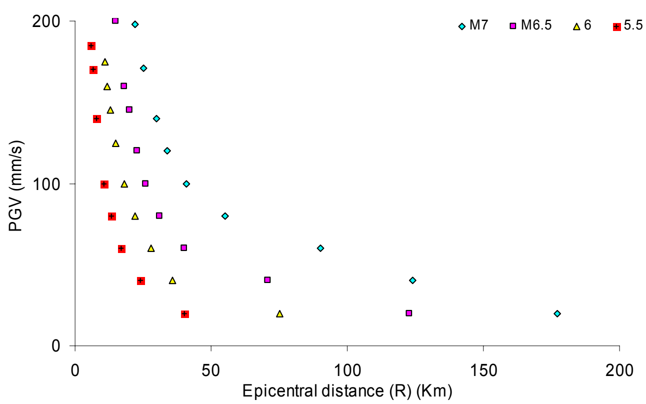


Figure 5. Earthquake scenarios with various magnitude distance (M-R) combinations for site class D soil.
∗ M: Magnitude of earthquake, R: Epicentral distance in Km ∗ PGV: Peak ground velocity in mm/s on rock (representing the intensity of hazard in the area).

## 4 PEAK DISPLACEMNT DEMAND

*Elastic systems: Simplified displacement response spectrum on rock and soil site*

The maximum spectral displacement ($RSD_{max}$) or peak displacement demand (PDD), on rock site for low and moderate seismic regions can be estimated in accordance with the second corner period

($T_2$) and the maximum response spectral velocity ($RSV_{max}$); where, $RSV_{max}$ can be obtained using equation 1:

$$RSV_{\max} = C(PGV) \quad (1)$$

where, C is the multiplying factor =1.8 for rock sites and PGV is peak ground velocity (Lam et al., 2000). $RSD_{max}$ can be obtained as the intersection of $T_2$ and ( $RSV_{\max} T / 2\pi$ ) (Figure 6a). where, $T_2$ is second corner period. $RSD_{max}$ can be considered as maximum displacement demand of linear elastic systems on rock site by using following equation 2:

$$RSD_{\max} = RSV_{\max} T_2 / 2\pi \quad (2)$$

where $T_2 = 0.5 + 0.5(M - 5)$ for rock site, M is the magnitude of earthquake


(a) Simplified displacement response spectrum on rock site (b) Simplified displacement response spectrum on soil site
Figure 6. Simplified displacement response spectrum.

It has been observed from the studies that displacement demand is amplified for soil sites (Figure 6b) and the amplification factor can vary between 4 and 6 (Venkatesan, S 2006). To sum up, RSD max on soil can simply be estimated to be amplification factor multiplied by RSD on rock site at site natural period ($T_g$).

## 5 SEISMIC ANALYSIS OF STRENGTH DEGRADED STRUCTURES

The single degree of freedom (SDOF) systems representing RBO, URM and SSC were subjected to nonlinear time history analyses with hysteretic models presented in section 2 and using various simulated accelerograms as presented in section 3. The maximum displacement demands of SDOF systems observed from time history analyses are compared with maximum displacement capacity of the structures. Results from the analyses were used to determine the state of failure of the structure. The computer program RUAUMOKO (Carr, 2003) and ROWMANRY (Doherty, 2002) were used to determine the maximum displacement demands for SSC, URM and RBO respectively. Fragility curves which define the probability of failure of the structure are then developed to predict the drift demand. The following paragraph describes the procedure for developing fragility curves.

Fragility curves were constructed based on the cumulative probability of exceedance function and the log normal distribution curve fitting function. Parameters used for constructing the fragility curves were estimated by the likelihood function (L) as expressed in equation 3.

$$L = \prod_{i=1}^{N} \left[F(d_i)\right]^{x_i} \left[1 - F(d_i)\right]^{1-x_i} \quad (3)$$

where $F(d_i)$ represents the cumulative distribution function(CDF) estimated at each RSD value. $x_i$ is 1 or 0 based on the failure state that corresponds to average RSD $_{max}$ and N is the total number of cases considered for the analysis. $F(d)$ is written in the analytical form as stated in equation 4.

$$F(d_i) = \Phi\left(\frac{\ln\left(\frac{d_i}{\mu}\right)}{\beta}\right) \tag{4}$$

where "$d$" represents RSD and $\Phi[]$ represents the log normal distribution function. The CDF evaluation is based on a unique value of $\mu$ and $\beta$ which are defined as the median and standard deviation value respectively. These unique values can be obtained by maximising the Likelihood function (equation 5).

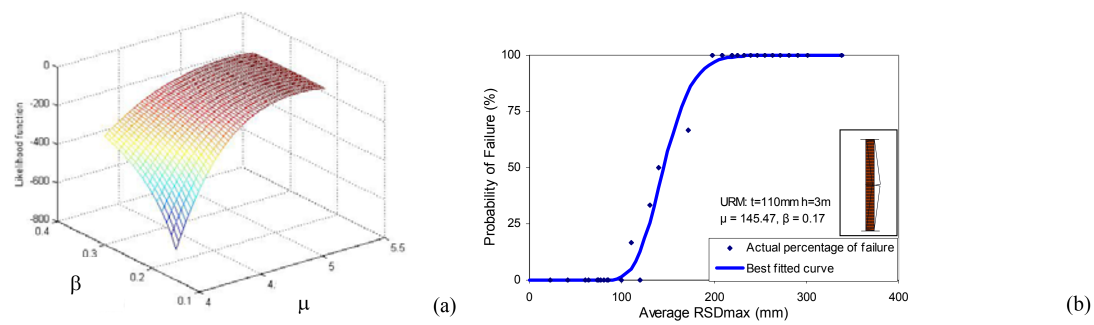


Figure 7. Development of fragility curve (a) determination of $\mu$ and $\beta$ using optimasation algorithm (b) fragility curve for URM (h=3m, t=0.11m-severe condition).

$$\frac{d \ln L}{d\mu} = \frac{d \ln L}{d\beta} = 0 \tag{5}$$

The procedure described by Shinozuka et al. (2001) was used for obtaining the best fit curve. The computation was performed by the optimasation algorithm which was implemented in MATLAB (Figure 7a). An example of such fragility curve is shown in Figure 7b for a URM structure (h=3m, thickness = 110mm, "severe" condition).

### 5.1 *Unreinforced masonry structures (URM)*

Single and double brick walls were considered for analyses; wall 1 and wall 2 were 110 mm and 230 mm in thickness. The displacement response of the structure in dynamic conditions of an earthquake was simulated by nonlinear time history analyses (THA). SDOF systems representing URM walls possessed force displacement relationships as described in section 2.2. The simulation of accelerograms was described in section 3. Fragility curves for aforementioned conditions were then generated. To investigate which seismic parameter (PGV or RSD $_{max}$) can best represent the probability of failure; wall 1 in the "new" condition was analysed for a range of M-R combinations for site class D (Figure 5). It is shown in figure 8a that fragility curves for representing the probability of failure of the walls were very inconsistent with simulations based on different earthquake magnitudes. Interestingly, the fragility curves became much more consistent when PGV was replaced by RSD $_{max}$ as the parameter for charaterising the intensity of ground shaking (Figure 8b).

Secondly it is important to investigate the effects wall height has upon the probability of failure. Walls ("new" and "severe" conditions) of different heights (2.5m, 3m, 3.5m having 110mm thickness) were analysed for M 7 earthquakes with varying epicentral distances. The outcome of the parametric study shows that when the height varied between 2.5 m and 3.5 m, no significant change in the fragility curves was observed (Figure 9 a,b).

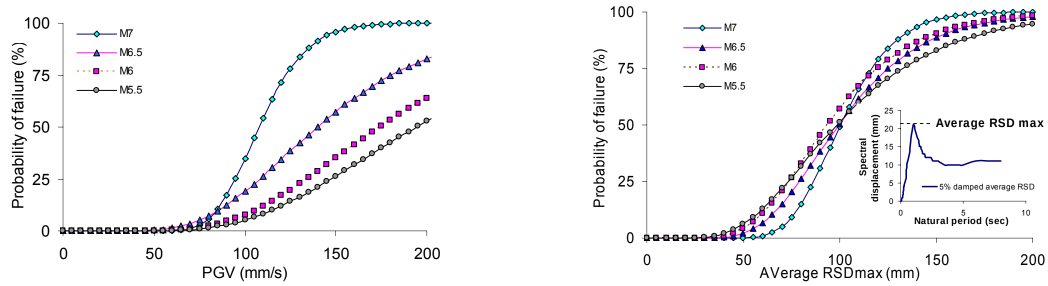


(a) PGV as parameter (b) RSD $_{max}$ as parameter

Figure 8. Fragility curves for URM walls (wall 1 "new", t=110mm, h=3000mm).

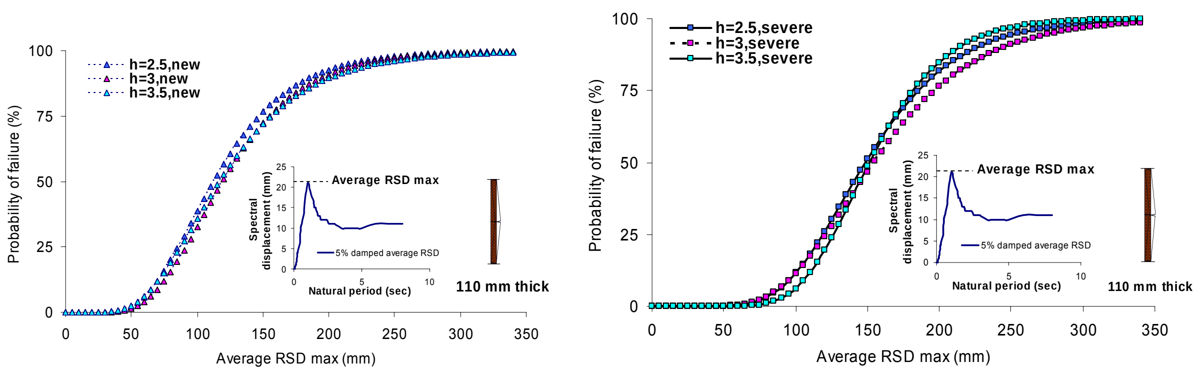


(a) "New" condition (b) "Severe" condition

Figure 9. Fragility curves for URM walls (wall 1: t=110mm, with h=2.5 m, 3 m, 3.5 m) for M7 earthquakes.

Wall 1 (110mm) and wall 2 (230mm) with different conditions of strength degradation and of height 3 m have also been investigated for their seismic performance. It is observed that, the strength degradation of the wall is shown to have not affected the probability of failure significantly (Figure 10 a, b).

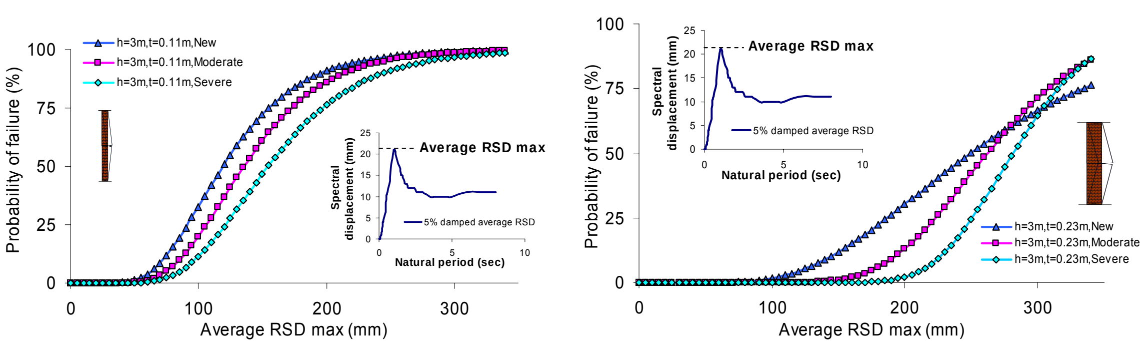


(a) wall 1: t=110mm (b) wall 2: t=230mm

Figure 10. Fragility curves for 3 m high URM walls of different thicknesses and conditions of degradation based on M7 earthquakes.

An interesting observation to make of Figure 10 is that the extent of strength degradation in the URM wall is shown not to have increased its probability of failure. The 5% probability of failure limit has been considered for recommendations. The drift demand of wall 1 and wall 2 is summarized in Table 2. The seismic hazard factor, z (g's) shown in Table 2 is between 0.09 to 0.12 which is comparable to the seismic hazard factor of some of the major places in Australia such as Adelaide, Newcastle (AS 1170.4-2007). Therefore, for 500 year return period the URM walls if properly constructed should be safe from overturning on onerous soil sites similar to the one which is considered in this paper (site natural period = 0.9 sec). For quick assessment, it is not unreasonable to take $RSD_{max}$ to be equal to 0.6 to 0.7 (i.e. two- thirds) of the wall thickness for design purposes.

Table 2: Seismic hazard factors for URM walls

| Thickness of wall (mm) | 5% probability of failure | | | |
|---|---|---|---|---|
| | $RSD_{max}$ on soil (mm) | M-R combination | Z (g's) | Factor |
| 110 | 65-85 | (M7-R85) – (M7-R30) | 0.09-0.12 | 0.6-0.8 |
| 230 | 125-215 | (M7-R34) – (M7-R21) | 0.18-0.31 | 0.6-0.9 |

$z(g's) = PGV(mm/s)/750$ , $PGV = RSV_{max(rock)}/1.8$

## 5.2 *Rigid body Objects (RBO)*

A free standing object such as computer cabinet or library steel rack in a building may be excited into rocking motion during an earthquake (Figure 11a). The research described in this paper is aimed at determining the displacement of these objects and developing fragility curves. A simple computer cabinet of 350 x 200 mm in size has been analysed for its response to ground shaking based on M7 events. The probability of failure has been plotted in Figure 11b. The value of $RSD_{max}$ corresponding to 5% probability of failure has been identified for design purposes. It has been observed from the fragility curve that this limiting value of $RSD_{max}$ was about two- thirds of the thickness of the object (Figure 11b). The research is ongoing on RBO of varying geometry. The POF of RBO decreases with increasing dimension (width) as reported by Al Abadi et al., 2006.

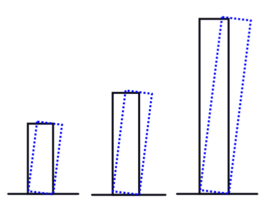

(a) Rocking objects

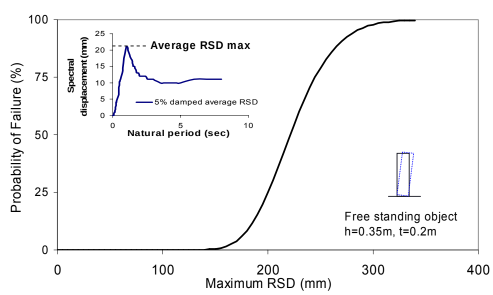


(b) Fragility curve

Figure 11. Free standing object subjected to M7 earthquake combinations.

## 5.3 *Soft storey structures*

### *Hysteretic modelling*

The values of parameters defining the hysteretic models were derived by curve fitting the models to the hysteretic loop recorded from cyclic testing. It has been found from calibration, that a reasonable match can be observed using the modified Takeda hysteretic model. Examples of a calibrated hysteretic model are presented in Figure 12a and 12b. The strength degradation parameters are defined in Figure 12d. The parameter (r) in modified Takeda model (Figure 12c) is rate of strength hardening which is taken as equal to zero in this study. The reasonable matches for unloading ($\alpha$) and reloading parameters ($\beta$) of modified Takeda hysteretic model are shown as below:

- For flexure dominated column: modified Takeda hysteretic model $\alpha$=0.5,$\beta$=0.2
- For shear dominated column: modified Takeda hysteretic model $\alpha$=0.5,$\beta$=0.6

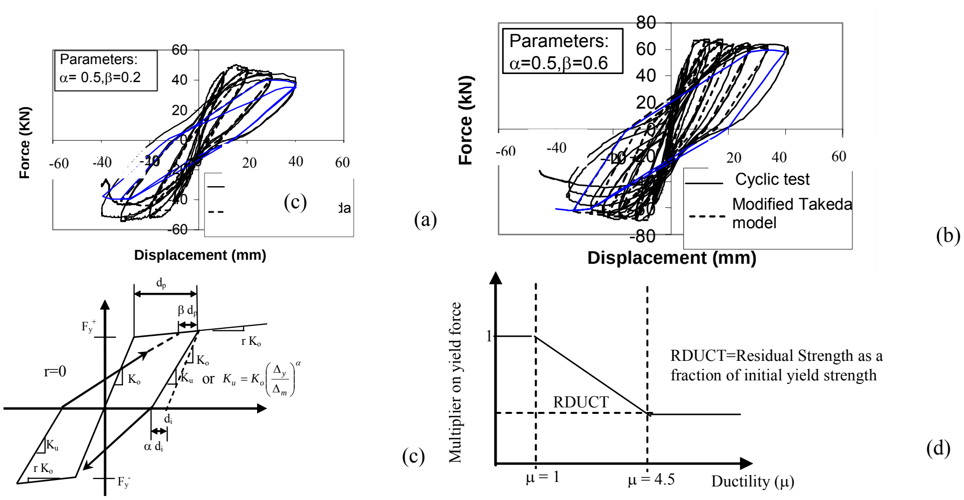


Figure 12. Cyclic test results for soft storey columns (a) flexure dominated column (b) shear dominated column (c) modified takeda model (d) strength degradation parameters.

The SDOF systems with hysteretic model representing soft storey column (Figure 12c) were then subjected to non linear time history analyses using ensembles of simulated accelerograms based on M7 events. A computer program RUAUMOKO is used for predicting the peak displacement demand. Results from the analyses were correlated with average RSD $_{max}$ for the construction of fragility curves which presented in Figure 13. It is shown that the drift demand of shear dominated columns is higher than that of flexural dominated columns. It is not the intention of this paper to generalize results at this stage. Research is ongoing on the potential seismic performance behaviour of soft storey columns possessing different dimensions.

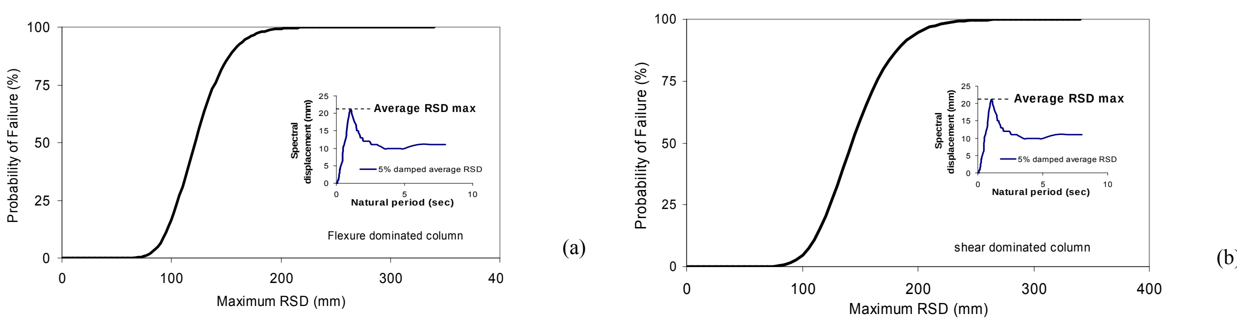


Figure 13. Fragility curves for soft storey columns subjected to M7- R combinations (a) flexural dominated column (b) shear dominated column.

## 6 CLOSING REMARK

This paper presents fragility curves for estimating the probability of failure of strength degraded components such as rigid body objects, unreinforced masonry structures and soft storey building structures. The fragility curves were developed based on hysteretic behaviour obtained from the cyclic testing for soft storey columns. The observed force displacement relationships have been presented. The simulated accelerograms used for analyses were generated using stochastic simulation considering different magnitude-distance combinations which represents both near-field and far-field earthquakes. More than 3000 time- history analyses have been undertaken to investigate the performance of strength degraded structures under various seismic conditions. The outcomes from the analyses reveal interesting results. The fragility curves associated with different earthquake magnitudes were found to be inconsistent when PGV was used to characterize the intensity of ground shaking. Parametric studies show that as the wall height varied from 2.5 to 3.5 m there was no significant change to the fragility curve. Moreover, strength degradation of the wall is shown to have not increased the probability of failure. For quick assessment, it is not unreasonable to take $RSD_{max}$ to be 0.6 to 0.7 (i.e. two- thirds) of the wall thickness or thickness of the rigid body object for design purposes. In other words the wall is deemed to be safe, as long as the $RSD_{max}$ is two-thirds of the thickness of wall. For 500 years return period, the URM walls, if properly constructed, should be safe from overturning on an onerous soil site similar to the one considered in this paper (site natural period = 0.9 sec). However, the analyses have not incorporated the filtering effects of the building. Hence, parapet walls at the roof of the buildings might be subjected to a level of hazard much higher than is shown on the fragility curves presented in the paper. It is also observed that shear dominated column has higher drift demand than flexural dominated column. Further research is needed to comment on quick assessment of a soft -storey column.

## 7 REFERENCES

Al Abadi, H., Lam, N., Gad, E., 2006. A simple displacement–based model for predicting seismically induced overturning, Journal of earthquake Engineering, 10(6).

AS/NZS 1170.4 2007. Structural Design Actions-Part 4 Earthquake Actions, Standards Australia, Sydney.

AS 3600, 2001. Australian standards for Concrete structures, Building code of Australia, Primary referenced standard.

ATC40 1996. Seismic Evaluation and Retrofitting of Concrete Buildings, Applied Technology Council, USA.

Carr, A. J. (2003) Ruaumoko, The Maori God of Volcanoes and Earthquake, University of Canterbury, New Zealand.

Doherty K., Griffith M. C., Lam, N., Wilson, J., 2002. Displacement – based seismic analysis for out – of – plane bending of unreinforced masonry walls. Earthquake Engineering and Structural Dynamics, Vol. 31: 833-850.

FEMA273 1997. NEHRP Guideline for the Seismic Rehabilitation of Buildings, Washington DC, Federal Emergency Management Agency, USA.

Idriss, IM & Sun, JI 1992. Users Manual for SHAKE-91. Sponsored by National Institute of Standards and Technology, Maryland USA and Dept. of Civil & Environmental Engineering, University of California, Davis, USA.

Lam, NTK first written: 1996 and latest edition: 1999. Program ETAMAC users' manual. Department of Civil & Environmental Engineering, University of Melbourne.

Lam, NTK first written: 1999 and latest edition: 2002. Program GENQKE users' manual. Department of Civil & Environmental Engineering, University of Melbourne.

Lam, NTK., Wilson, JL., & Hutchinson, GL 2000. Generation of synthetic earthquake accelerograms using seismological modelling: a review. Journal of Earthquake Engineering 4(3): 321-354.

Lam, N., Griffith M., Wilson, J., and Doherty. 2003. Time-history analysis of URM walls in out of plane flexure. Engineering Structures, Vol. 25:743-754.

Lam, N., & Chandler, A. 2005. Peak displacement demand of small to moderate magnitude earthquake in stable continental regions, Earthquake Engineering and Structural Dynamics, 34: 1047-1072.

Lam, N., Wilson, J., Venkatesan, S. 2005. Accelerograms for dynamic analysis under the new Australian Standard for earthquake actions. Electronic Journal of Structural Engineering, Vol. 5: 10-35.

Rodsin, K., Lam , N., Wilson, J., Goldsworthy, H. Shear controlled ultimate behaviour of non ductile reinforced concrete columns, Australian Earthquake Engineering Society proceeding of the 2004 conference, Mount Gambier , South Australia.

Rodsin, K., Lam , N., Wilson, J., Goldsworthy, H. Collapse behaviour of columns with low aspect ratios, 19th Australian Biennial Conference on the Mechanics of Structures and Materials, University of Canterbury, Christchurch, New Zealand 2006 .

Shinozuka, M., Feng, M Q., Kim, H., Uzawa T., Ueda, T. 2001. Statistical analysis of fragility curves, Technical Report MCEER, Department of Civil and Environmental Engineering, University of Southern California, Task Numbers 106-E-7.3.5 and 106-E-7.6.

Venkatesan, S 2006. A soil amplification model for intra-plate seismic regions, PhD Thesis. Department of Civil & Environmental Engineering, University of Melbourne.